Available online at www.sciencedirect.com
ScienceDirect
Solid-State Electronics 51 (2007) 333–336
SOLID-STATE ELECTRONICS
www.elsevier.com/locate/sse

Towards Si-based photonic circuits: Integrating photonic crystals in silicon-on-insulator platforms

G. Kocher [a,*], W. Khunsin [a], S. Arpiainen [b], J. Romero-Vivas [a], S.G. Romanov [a], J. Ye [c], B. Lange [c], F. Jonsson [a,1], R. Zentel [c], J. Ahopelto [b], C.M. Sotomayor Torres [a]

[a] *Tyndall National Institute, University College Cork, Lee Malting, Cork, Ireland*
[b] *Technical Research Centre of Finland, VTT Information Technology, P.O. Box 1202, FIN-02044 VTT, Finland*
[c] *Department of Chemistry, University of Mainz, Duesbergerweg 10-14, D-55099 Mainz, Germany*

The review of this paper was arranged by Raphaël Clerc, Olivier Faynot and Nelly Kernevez

Abstract

In the context of Si-based photonics, we report on a strategy to integrate two optical components, a 3D photonic crystal light emitter and a waveguide, in a silicon-on-insulator patterned substrate. Self-assembled colloidal photonic crystals are produced with high crystalline quality and spatial selectivity. Plane wave expansion and finite-difference time-domain have been used to find suitable configurations for positioning emitters and waveguides. The first steps toward the realisation of these configurations are presented.

PACS: 42.70.Qs; 42.82.Fv; 83.80.Hj

Keywords: Photonic crystals; SOI; Silicon

1. Introduction

The advantages of photonic crystals over classical optical materials hold the promise of ultra-compact optical component to, for example, guide light and control the spontaneous emission. Nevertheless, the challenges faced range from the understanding of physical phenomena to strategies to couple components in order to integrate them on a technologically relevant platform.

While silicon-on-insulator (SOI) photonic crystal (PhC) waveguides are relatively well understood and their fabrication has been optimised [1], their integration with other optical elements on a photonic platform remains elusive due to (a) the stringent fabrication needs to obtain state of the art (low loss) PhC waveguides and (b) the absence of realistic coupling strategies which necessarily must include matching of modes in both components. One key feature of 3D PhCs is the possibility of enhancing or inhibiting spontaneous emission depending on whether the emission frequency falls within the photonic band gap or not. It has been shown that the directional properties of the spontaneous emission from opal-based PhCs can be modified [2]. The combined advantages of both controlled spontaneous emission and directionality justify the use of 3D PhCs for this integration approach.

For the realisation of photonic building blocks and their integration, it is necessary to find a way to place the crystals on a specific position on the wafer. Spatial selectivity is realised by sedimentation of colloidal crystals on pre-patterned cavities on a patterned SOI substrate [3]. The method is used in a first instance to integrate a tapered rib waveguide and a 3D PhC light emitter. In parallel, FDTD simulations are carried out to determine the mode

* Corresponding author. Tel.: +353 214904433; fax: +353 214904467.
E-mail address: Gudrun.kocher@tyndall.ie (G. Kocher).
[1] Present address: School of Physics and Astronomy, University of Southampton, SO17 1BJ, United Kingdom.

0038-1101/$ - see front matter © 2007 Elsevier Ltd. All rights reserved.
doi:10.1016/j.sse.2007.01.010

structure of the PhC emitter in order to ensure mode matching between the waveguide and the emitter.

2. Sedimentation of 3D photonic crystals on patterned substrates

The opal photonic crystals were self-assembled on pre-patterned SOI substrates, from a 2 mass percent dispersion of poly(methyl methacrylate) (PMMA) spheres in de-ionised water or a 2 mass percent dispersion of silica beads in de-ionised water. The PMMA spheres were fabricated with a diameter of $a = 370$ nm using the modified surfactant free emulsion polymerisation technique [4,5]. The silica beads were purchased from Bangs Laboratories and had a mean diameter of 880 nm. The pattern on the substrate was defined by UV lithography and etched in an inductively coupled plasma (ICP) reactor using fluorine chemistry. The pattern was etched all through the SOI top layer (see Fig. 1, right). The depth of the pattern depended on the thickness of the SOI top layer, which ranged from 5 to 10 μm. The structures on the pre-patterned substrates were completely filled, so the thickness of the films corresponds to the etching depth of the structures. Therefore, with a bead diameter of $a = 370$ nm, the PMMA opals consist of 15 or 30 layers, respectively. In the case of 3D silica opals, the resulting PhCs consist of 6–11 layers. Typical structures are shown in Figs. 1 and 3.

The sedimentation is carried out by a variation of the vertical deposition technique [6] as illustrated in Fig. 2. The substrate is slowly drawn from the suspension of de-ionised water and PMMA beads while an acoustic field is applied in the form of white noise. The formation of the face-centred cubic (fcc) lattice of the opal takes place at the meniscus formed at the suspension-air interface.

The form and size of the meniscus is highly dependent on the hydrophilic or hydrophobic nature of the substrate surface. Only a hydrophilic surface will lead to the formation of a meniscus and subsequent crystal growth [7]. The patterned substrates used in this work offer various combinations of hydrophobic and hydrophilic surfaces for the bottom and sidewalls of the pre-defined sedimentation wells. If the parameters are chosen correctly, wherever there are grooves, the growth is initiated earlier than in flat areas, leading to site selectivity of the growth process as shown in Fig. 3. We found that a pattern on SOI wafers with a hydrophilic bottom surface in the sedimentation trenches made up by the top of the SiO_2 Box layer, and hydrophobic side wall surfaces formed by the crystalline SOI top layer (see Fig. 1, right) results in the best crystalline quality for the sedimented opals.

The magnitude of the acoustic field is chosen in a way that keeps the spheres unsettled without destroying the meniscus. The acoustic vibrations help re-organising non-systematic cracks into systematic ones. Moreover, plane-stacking faults, while being the most common defects observed opals structures [8], are practically absent from our samples. The resulting structures on unpatterned Si substrates show an impressive fcc arrangement free of distortion throughout the whole sample (see Fig. 2) [9].

The effect of acoustic vibrations on the quality improvement of the structure has been tentatively related to the stochastic resonance mechanism [10]. Theoretical investigations showed, that the free energy values for hcp and fcc lattices are very close together with the fcc lattice configuration slightly lower in energy, i.e., slightly more favourable, but both phases are highly likely to coexist [11]. The acoustic disturbance in our set-up gives the beads more time to settle, thereby enhancing the probability to reach the overall energy minimum of the system, which is represented by the fcc configuration. The quantitative details of this mechanism will be described elsewhere [12].

3. Simulations

For a fcc lattice configuration, a full gap can open between the 8th and the 9th bands for sufficiently high refractive indices, which is rather small and sensitive to the presence of defects [13]. In opal-based PhCs, this requires the structure to be inverted with a high index material, namely silicon. The next step towards integration and hybrid structures is defect engineering in 3D PhCs, to incorporate functional device-like structures.

In principle one can think of all kind of defects, starting from point [14] to linear [15] and 2D defect lattices [16]. However, as in classic semiconductors, defects are needed for propagation and coupling of electromagnetic waves. The preparatory work for defect incorporation has been realised [17] and is currently being optimised. We target

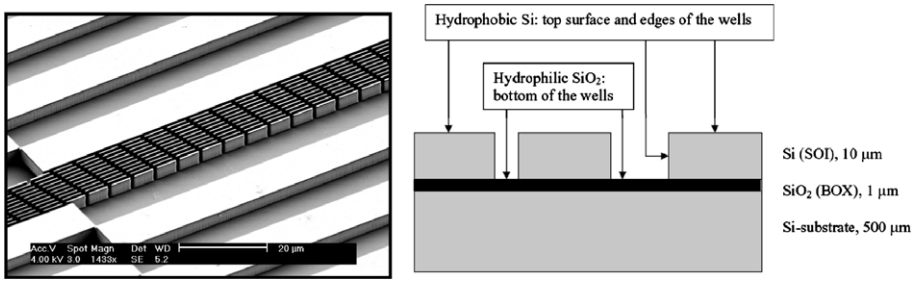

Fig. 1. Left: SEM micrograph of pre-patterned SOI substrate. Right: schematics of SOI substrate with varying hydrophilic and hydrophobic surface states.

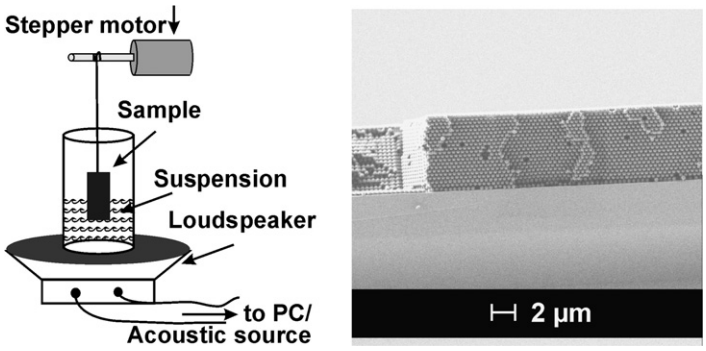

Fig. 2. Left: Schematic drawing of acoustic vibrations assisted variation of vertical growth deposition. Right: SEM micrograph of a PMMA opal with bead diameter 370 nm showing the high crystalline quality and perfect fcc configuration.

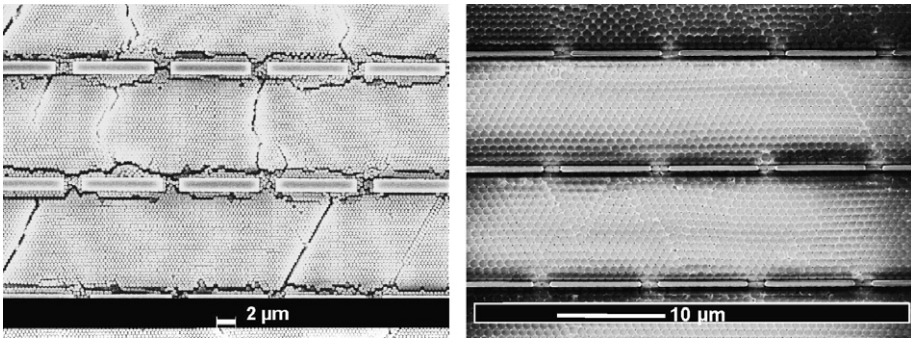

Fig. 3. SEM micrograph showing the crystalline quality and site selectivity of the grown photonic crystals. Left: PMMA opals with bead diameter 370 nm. Right: silica opals with a sphere diameter of 880 nm.

the emission at 1.5 μm, where silicon-inverted opal PhC doped with Erbium ions represents a possible route for emission. Si-inversion, by chemical vapour deposition growth and subsequent calcinations, has been obtained and is undergoing characterisation.

We use electron-beam (e-beam) lithography to inscribe individual point defects acting as cavity and superlattices of point defects on a 3D photonic colloidal (PMMA) crystal by selective exposure of single beads and subsequent development. These defects on the 3D opal could serve as a template for the formation of both a buried defect as well as for a double inversion process, that results in a silicon inverted opal. Starting with a first sedimentation and sintering of the crystal, the uppermost layer of beads could be inscribed with the designed defects. After a second deposition and subsequent sintering, the whole structure would be developed resulting in a buried defect layer. Furthermore, the PMMA opals could serve as a template for a double inversion process [18].

The modelling work for these structures is based on the plane-wave expansion for the determination of the band structures and on 3D finite-difference time-domain (FDTD) for the study of the mode structure of the emitter in a cavity (defect) and transmission data in the 3D PhC. These defects can be used to enhance spontaneous emission and thus produce light with a modified spectrum directed to the output waveguide. Fig. 4 shows the mean value of the Poynting vector as a function of normalised frequency Ω at a point near the centre of a silicon sphere in an inverse silicon opal. The structure is scaled for doping of the sphere with Erbium, leading to a lattice constant a of 1,26 μm and the sphere diameter is 893 nm.

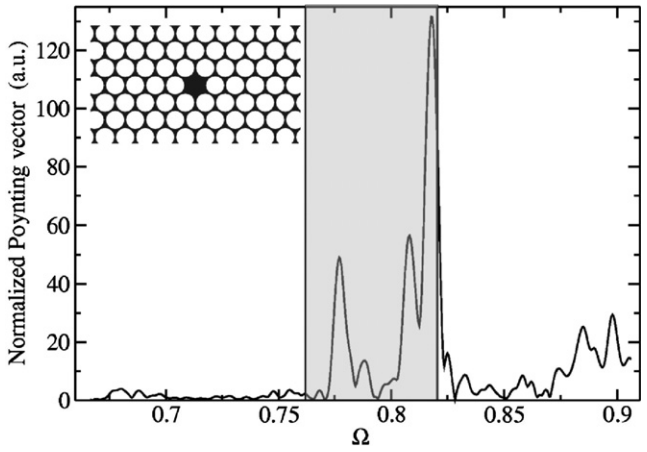

Fig. 4. Cavity made removing completely an air sphere. The figure shows the spectrum of the mean value of the Poynting vector in a point near the centre of a sphere in an inverse silicon opal. The spectrum was normalized against a reference run in vacuum. The vertical lines mark the position of the bandgap, the insert shows a schematic of the simulated structure.

Patterning polymer opals with electron beam lithography differs significantly from patterning spin-coated flat

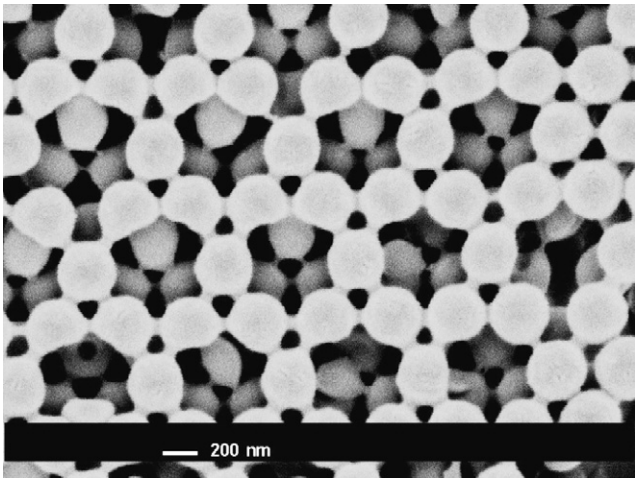

Fig. 5. SEM Micrograph of defect lattice produced by e-beam lithography on PMMA opal (bead diameter 370 nm). The opal was grown on a pre-patterned substrate.

substrates. The write field effectively gains another degree of freedom, since only with suitable electron beam parameters, the uppermost layer of the opal is selectively exposed while the layer immediately beneath remains undisturbed. Therefore, the exposure depth becomes a crucial parameter controlled by the acceleration voltage of the electron beam, which in turn controls both the penetration depth as well as the transverse extent of the cloud of scattered electrons inside the individual beads. Fig. 5 shows a hexagonal superlattice of defects inscribed on a 3D PMMA opal. For 370 nm bead diameter, the optimum acceleration voltage was found to be 4 kV with a dose of 50 $\mu C/cm^2$.

4. Conclusions

We report progress in the quest of integrated PhC-based optical components in SOI platforms. The initial engineering stages of physical integration of the components have been developed by fabricating opals with high crystalline quality and spatial selectivity. We have shown that applying an acoustic field during growth enhances the crystalline quality. Pre-patterned substrates with suitable surface treatments provide templates for the spatially selective growth. The study of mode structures for a 3D PhC emitter is the next step to design and fabricate a mode-matched rib waveguide and light emitter. Plane wave expansion and FDTD have been used to determine appropriate structures and first steps towards the realisation of integrated optical components are taken. This approach, if successful, will open the door to compact silicon-based photonic circuits.

Acknowledgements

Project supported by the Science Foundation Ireland, the EU IST FET Project No. 510162 (PHAT), the Academy of Finland Project No. 53942, the EU NoE 511616 (PHOREMOST), the EU thematic network EUROSOI and the German Research Society (DF6).

References

[1] Vlasov YA, O'Boyle M, Hamann HF, McNab SJ. Nature 2005:438.
[2] Romanov SG, Chigrin DN, Sotomayor Torres CM, Gaponik N, Eychmuller A, Rogach AL. Phys Rev E 2004;69:046606.
[3] Ferrand P, Minty MJ, Romanov SG, Sotomayor Torres CM, Egen M, Zentel R, et al. Nanotechnology 2003;14:323.
[4] Müller M, Zentel R, Maka T, Romanov SG, Sotomayor Torres CM. Chem Mater 2000;12:2508.
[5] Egen M, Zentel R. Chem Mater 2000;14:2176.
[6] Gu ZZ, Fujishima A, Sato O. Chem Mater 2002;14:760.
[7] Fustin CA, Glasser G, Spiess HW, Jonas U. Langmuir 2004;20:9114.
[8] Vlasov YA, Astratov VN, Baryshev AV, Kaplyanskii AA, Karimov OZ, Limonov MF. Phys Rev E 2000;61:5784.
[9] Von Rhein E, Bielawny A, Greulich-Weber S. MRS Symp Proc 2006:901.
[10] Shinbrot T, Muzzlo FJ. Nature 2001;251:410.
[11] Pronk S, Frenkel D. J Chem Phys 1999;110:4589.
[12] Amann A, Khunsin W, Kocher G, O'Reilly E, Sotomayor Torres CM (to be published).
[13] Lin ZY, Zhang ZQ. Phys Rev B 2000;62:1516.
[14] Jun Y, Leatherdale CA, Norris DJ. Adv Mater 2005;17:1908.
[15] Vynck K, Cassagne D, Centeno E. Optics Express 2006;14(15):6668.
[16] Chutinan A, John S. Phys Rev E 2005;71(2):026605.
[17] Jonsson F, Sotomayor Torres CM, Seekamp J, Schniedergers M, Tiedemann A, Ye J, et al. Microelectron Eng 2005;78–79:429.
[18] Gratson GM, García-Santamaría F, Lousse V, Xu M, Fan S, Lewis JA, et al. Adv Mater 2005;18(3):461.